J. Fluid Mech. (1973), *vol.* 57, *part* 4, *pp.* 753–767
Printed in Great Britain

Time-dependent shear flows of a suspension of particles with weak Brownian rotations

By E. J. HINCH
Department of Applied Mathematics and Theoretical Physics, University of Cambridge

AND L. G. LEAL
Chemical Engineering, California Institute of Technology, California 91109

(Received 11 October 1972)

A dilute suspension of rigid axisymmetric particles in a time-dependent shear flow is considered in circumstances where the shear flow alignment of the particles dominates small but not unimportant Brownian disorientations. Three cases are studied: stress relaxation on the cessation of a steady shear, the sudden application of a steady shear from a state of rest and the sudden change from one steady shear rate to another. The rheology exhibits effects on two basic time scales provided that the particle aspect ratio r is not extreme: oscillatory features with a frequency proportional to the shear rate γ which are due to the rotation of the particles about their Jeffery orbits, and an exponentially fading memory due to Brownian diffusion with a characteristic time proportional to the inverse diffusion rate D^{-1}. When the particle aspect ratio r becomes large, the oscillation frequency is reduced to γ/r while the diffusion rate is enhanced to Dr^2 for some features and to Dr^4 for others.

1. Introduction

In this paper we continue our investigation of a suspension of particles whose orientation is affected by Brownian rotations. Attention is restricted to a dilute suspension of rigid spheroidal particles which are free of external forces or couples and which also are sufficiently small that inertia is negligible in the microscale mechanics. The constitutive relation for this suspension consists of three equations as we shall now recall.

When placed in a linear bulk flow composed of a symmetric strain rate $\mathbf{E}$ and an antisymmetric vorticity $\mathbf{\Omega}$,

$$\mathbf{u}(\mathbf{x},t) = [\mathbf{E}(t)+\mathbf{\Omega}(t)].\mathbf{x},$$

an isolated particle will rotate in the absence of Brownian couples such that the unit vector $\mathbf{p}(t)$ in the direction of its symmetry axis changes according to

$$\dot{\mathbf{p}} = \mathbf{\Omega}.\mathbf{p}+(r^2-1)(/r^2+1)[\mathbf{E}.\mathbf{p}-\mathbf{p}(\mathbf{p}.\mathbf{E}.\mathbf{p})], \tag{1}$$

where r is the particle aspect ratio. The random Brownian motions require the introduction of a differential probability density function $N(\mathbf{p},t)$ to describe the particle's orientation. The evolution of $N(\mathbf{p}, t)$ with time is governed by a simple Fokker–Planck equation

$$(\partial N/\partial t) + \operatorname{div}(N\dot{\mathbf{p}} - D\nabla N) = 0. \tag{2}$$

The first contribution to the probability flux is an undisturbed advection given by (1). The Brownian motions contribute an additional flux which is modelled as a diffusion process with a Stokes–Einstein diffusion coefficient D. The bulk stress consists of a Newtonian term $2\mu\mathbf{E}$ for the pure solvent, plus a contribution

$$\boldsymbol{\sigma} = 2\mu\Phi\{A\langle\mathbf{pppp}\rangle : \mathbf{E} + B[\langle\mathbf{pp}\rangle . \mathbf{E} + \mathbf{E} . \langle\mathbf{pp}\rangle] + C\mathbf{E} + F\langle\mathbf{pp}\rangle D\}. \tag{3}$$

Here μ is the viscosity of the suspending fluid, Φ the volume fraction of the particles and A, B, C and F material coefficients which depend only on the particle aspect ratio and shape and are given for spheroids in Hinch & Leal (1972). The angled brackets denote averages of the included quantities weighted with the distribution function N. The last term in (3) is known as the diffusion stress, about whose inclusion there is some debate, and the rest as the strain stress.

It is apparent that the constitutive relations, equations (1)–(3), are mathematically complex despite the simplicity of the physical model. Except for the immediate observation of nonlinearity and a fading memory, little can be said about the rheological behaviour in a general time-dependent linear flow. An understanding of the suspension must be obtained by piecing together numerous approximate solutions. This study is addressed to the time-dependent effects for shear flows in the limiting case of weak Brownian rotations (flows with strong shear).

We have previously tackled steady shear flows with weak Brownian motions, see Hinch & Leal (1972). Coupled with the earlier work for dominant Brownian rotations, that approximate solution allowed a complete picture (i.e. for all shear rates) of the shear-dependent intrinsic viscosity and normal stress differences. The asymptotic expansion which we developed in that paper will be extended here to deal with time variations of the bulk flow.

The constitutive equations (1)–(3) usefully simplify for nearly spherical particles. In an application of the simplified form to a variety of time-dependent problems (Leal & Hinch 1972) we identified two temporal characteristics of the suspension's rheology. First we noted that the near-sphere suspension acts as a natural oscillator with a frequency equal to, or half, the magnitude 2Ω of the vorticity. These oscillations originate in the oscillating flow seen by the effectively spherical particles as they spin with the vorticity. The other characteristic was an exponentially fading memory which is caused by the Brownian diffusion, and has a single time constant $6D$. In an oscillating flow with an imposed frequency ω, these two effects would typically combine to produce a linear impedance containing factors like $(\omega \pm \Omega + i6D)^{-1}$.

The present study attempts to determine how these two temporal characteristics become modified for strictly non-spherical particles. If Brownian motions dominate, the exponential decay swamps the oscillation. The suspension further remains nearly isotropic, so that the single decay rate is the same as that for the near-sphere limit, $6D$. When the Brownian motions are weak the situation is quite different. The oscillations have a much shorter time scale than the decay and hence can be seen before they decay away. We shall find that the anisotropy of the suspension associated with the particles' non-spherical shape can lead to quantitative changes in both the oscillation and its decay compared with the near-sphere model in the same limit, $D/\gamma \ll 1$.

2. Stress relaxation

Before proceeding to the analysis of general time-dependent shear flows with weak Brownian effects, we consider the trivial case of stress relaxation from a strong steady shearing flow

$$\mathbf{u}(\mathbf{x},t) = (\gamma(t)\,x_2, 0, 0),$$

$$\gamma(t) = \begin{cases} \gamma = \text{constant}, & t < 0, \\ 0, & t > 0. \end{cases} \tag{4}$$

The generalization of our near-sphere solution for this standard experiment can be given for arbitrary aspect ratios.

When the strain rate vanishes, evaluation of the bulk stress (3) only requires the calculation of the second moment of $\mathbf{p}$ with respect to N. In the absence of any flow the second moment can be obtained directly without recourse to the full distribution function. Multiplying (2) by $\mathbf{pp}$ and integrating over the orientation space produces

$$((\partial/\partial t) + 6D)\langle \mathbf{pp} - \tfrac{1}{3}\mathbf{I}\rangle = 0.$$

Substituting the solution of this equation into the expression (3) for the bulk stress yields

$$\boldsymbol{\sigma}(t) = 2\mu\Phi DF\langle \mathbf{pp} - \tfrac{1}{3}\mathbf{I}\rangle|_{t=0-}\,.\,e^{-6Dt} \quad (t \geqslant 0). \tag{5}$$

The three initial values of $\langle \mathbf{pp} - \frac{1}{3}\mathbf{I}\rangle$ associated with the shear stress and the two normal stress differences can be found as functions of the aspect ratio in table 3 of Hinch & Leal (1972) for the relaxation from a steady strong shear.

The main features of the rheological response in the present case of non-spherical particles are little changed from the results found in our previous investigation of the near-sphere suspension for this same flow. In that instance we found that the particle contribution to the bulk stress relaxed exponentially with a decay rate $6D$ after first suffering a discontinuous reduction in magnitude at the initial instant due to the vanishing of the strain-stress contribution for $\mathbf{E} = 0$. According to (5), the relaxation rate $6D$ and the initial drop in the particle contribution to the bulk stress are maintained in the present case. The main difference is the increase in the magnitude of the discontinuity in the normal stress for extreme aspect ratios, e.g. for rods, $r \gg 1$,

$$\frac{\sigma_{11}-\sigma_{33}}{\Phi\mu\gamma} = \begin{cases} 0{\cdot}25\dfrac{r^4}{\ln r}\dfrac{D}{\gamma} & (t = 0-), \\[2ex] 6\dfrac{r^2}{\ln r}\dfrac{D}{\gamma} & (t = 0+). \end{cases}$$

This is a consequence of the slow part of the orbit, which amplifies the strain stress relative to the diffusion stress.

The suspension is anisotropic for non-spherical particles in strong shear flow, with large gradients in the orientation distribution. These enhance the diffusional relaxation of the orientation distribution. The reason why the decay rate of the stresses does not similarly increase is that the diffusion stress (the only non-zero contribution when the strain rate vanishes) depends only on the second harmonic of the distribution. We shall see that the decay rate is modified when the bulk flow does not vanish.

3. The expansion for strong shear flows

We now set up the general asymptotic expansion which is required for time-dependent shear flows with weak Brownian effects. It will be necessary to restrict the varying shear flow to be strong at all times, i.e. $|\gamma(t)/D| \gg 1$. This unfortunately excludes oscillating flows which momentarily vanish.

The full equations (2) with (1) are first expressed in terms of the natural non-orthogonal C,τ co-ordinates defined in Leal & Hinch (1971):

$$\frac{\partial}{\partial t}\left(\frac{N}{g}\right)+\frac{r\gamma(t)}{r^2+1}\frac{\partial}{\partial \tau}\left(\frac{N}{g}\right) = Dg^{-1}\nabla^2_{C,\tau}N$$

$$= D\left\{\frac{\partial}{\partial C}\left[\frac{k}{h\sin\alpha}\frac{\partial N}{\partial C}-\cot\alpha\frac{\partial N}{\partial \tau}\right]+\frac{\partial}{\partial \tau}\left[\frac{h}{k\sin\alpha}\frac{\partial N}{\partial \tau}-\cot\alpha\frac{\partial N}{\partial C}\right]\right\} \quad (6)$$

with $g = (hk\sin\alpha)^{-1}$. Here the metric functions h, k and α are respectively the measures of length along the curves of constant τ and C and the angle of skewness between these curves. They are known functions of C and τ. Undisturbed by Brownian rotations the particles traverse one of a singly infinite family of closed periodic Jeffery orbits. The variable C specifies the particular orbit for a given particle, and τ the phase about that orbit. The combination g of the metric functions represents the concentration of probability due to the local slowing of the orbit speed and the crowding with nearby orbits.

Without a change in notation it is useful to declare the problem (6) non-dimensionalized with respect to some typical shear rate. Henceforth t will be a dimensionless variable, $\gamma(t)$ an $O(1)$ non-dimensional function and D a small dimensionless parameter.

As we have already noted, there exist two intrinsic time scales for changes in the orientation distribution. From the left-hand side of (6) there is one corresponding to the instantaneous orbit period $2\pi(r+r^{-1})/\gamma(t)$. From the right there is the diffusional time scale D^{-1}. In the limit of strong shear being considered here these two scales become very different: the orientation distribution shows rapid oscillations with a slow diffusion-induced drift. In order to obtain an asymptotic expansion in the small parameter D which is uniformly valid in time, we therefore employ the familiar method of 'two-timing'. Formally we introduce the long second time $T = Dt$, which is treated as a new independent variable. Thus the time derivative in (6) is replaced by

$$(\partial/\partial t)+D(\partial/\partial T).$$

Substituting the expansion for N,

$$N(C,\tau;\,t,T) = N_0 + DN_1 + D^2N_2 + \ldots,$$

into (6) and collecting together terms of like order in D produces the set of equations

$$\frac{\partial}{\partial t}\left(\frac{N_0}{g}\right) + \frac{r\gamma}{r^2+1}\frac{\partial}{\partial \tau}\left(\frac{N_0}{g}\right) = 0 \quad \text{to} \quad O(1), \tag{7a}$$

$$\frac{\partial}{\partial T}\left(\frac{N_0}{g}\right) + \frac{\partial}{\partial t}\left(\frac{N_1}{g}\right) + \frac{r\gamma}{r^2+1}\frac{\partial}{\partial \tau}\left(\frac{N_1}{g}\right) = g^{-1}\nabla^2_{C,\tau} N_0 \quad \text{to} \quad O(D), \tag{7b}$$

and so on to higher orders.

To simplify the advection operator on the left-hand side of equations (7) we transform variables from (t,τ) to (τ_0,τ), defining

$$\tau_0(t,\tau) = \tau - \int_0^t \frac{r\gamma(t')}{r^2+1}\,dt'.$$

We note that the previously stated restriction that $\gamma(t)$ should be single-signed ensures that this transformation has a well-defined unique inverse $t(\tau_0,\tau)$. In the new variables equations (7) become

$$\frac{r}{r^2+1}\gamma(\tau_0,\tau)\frac{\partial}{\partial \tau}\left(\frac{N_0}{g}\right) = 0, \tag{8a}$$

$$\begin{aligned}\frac{\partial}{\partial T}\left(\frac{N_0}{g}\right) &+ \frac{r}{r^2+1}\gamma(\tau_0,\tau)\frac{\partial}{\partial \tau}\left(\frac{N_1}{g}\right)\\ &= g^{-1}\nabla^2_{C,\tau,\tau_0}(N_0)\\ &= \frac{\partial}{\partial C}\left[\frac{k}{h\sin\alpha}\frac{\partial N_0}{\partial C} - \cot\alpha\left(\frac{\partial}{\partial \tau}+\frac{\partial}{\partial \tau_0}\right)N_0\right]\\ &\quad + \left(\frac{\partial}{\partial \tau}+\frac{\partial}{\partial \tau_0}\right)\left[\frac{h}{k\sin\alpha}\left(\frac{\partial}{\partial \tau}+\frac{\partial}{\partial \tau_0}\right)N_0 - \cot\alpha\frac{\partial N_0}{\partial C}\right].\end{aligned} \tag{8b}$$

The solution of the expansion now proceeds as follows. Equation (8a) is first integrated to obtain

$$N_0 = f_0(C,\tau_0,T)\,g(C,\tau). \tag{9}$$

This simply describes the undisturbed advection of the particles about fixed Jeffery orbits C. Depending on its initial phase τ_0, each particle changes its phase around the orbit according to

$$\tau = \tau_0 + \int_0^t \frac{r}{r^2+1}\gamma(t')\,dt'.$$

The distribution function is compressed by the geometry and speed of rotation about the orbits according to the factor g. The slow drift in the orientation distribution represented by the dependence of f_0 on T is undetermined at this stage because diffusion has not yet entered the calculation.

With f_0 temporarily unknown we proceed to the next approximation (8b), which now may be expressed as

$$\frac{\partial f_0}{\partial T} + \frac{r}{r^2+1}\gamma(\tau_0,\tau)\frac{\partial}{\partial \tau}\left(\frac{N_1}{g}\right) = g^{-1}\,\nabla^2_{C,\tau,\tau_0}(f_0 g).$$

This equation splits into two parts: a fluctuating part for the forcing of short-time variations in N_1 and a secular part which provides a constraint on f_0. The split comes from noting that N_1 must be single-valued in the periodic phase variable τ. Thus

$$N_1 = g(C,\tau)\left\{f_1(C,\tau_0,T)+\frac{r^2+1}{r}\int_0^{\tau}\frac{g^{-1}\nabla^2_{C,\tau,\tau_0}(f_0g)-\partial f_0/\partial T}{\gamma(\tau_0,\tau)}\,d\tau\right\} \tag{10}$$

and

$$\frac{\partial f_0}{\partial T} = \int_0^{2\pi}\frac{g^{-1}\,\nabla^2_{C,\tau,\tau_0}(f_0g)}{\gamma(\tau_0,\tau)}\,d\tau\bigg/\int_0^{2\pi}\frac{d\tau}{\gamma(\tau_0,\tau)}. \tag{11}$$

Equation (11) determines the way the first approximation to the distribution drifts under the action of the cumulative effects of weak Brownian couples. In the second approximation (10) the undetermined f_1 will be similarly constrained by an integral condition found from the N_2 problem. Our expansion procedure is again seen to be inapplicable to shear flows which momentarily vanish.

Although in principle any time-dependent strong shear flow can be tackled by (11), for most flows this would not be easy. The essential trouble lies in obtaining explicitly the inverse of the $\tau_0(t,\tau)$ transformation. This is required when performing the τ integrations in (10) and (11) at fixed τ_0. Associated with this mathematical complexity is the difficulty of physically comprehending the material response when the time variations of the imposed shear are not commensurate with the orbit's natural nonlinear oscillations. We have therefore only applied the general expansion to the transients of two steady strong shear flow problems: the start from the rest state and the step increase or decrease in shear rate. These flows are of special interest in view of their common application in experimental rheology.

4. An eigenvalue problem for steady shear flows

The eigenvalue problem associated with (11) can be usefully studied in isolation. The results will be employed in both the specific examples. When $\gamma(t)$ is a constant, the τ_0 transformation and the required integrals greatly simplify. Equation (11) becomes

$$2\frac{\partial f_0}{\partial T} = \frac{\partial}{\partial C}\left\{[HC^4+KC^2+M]\frac{\partial f_0}{\partial C}+[2HC^4+(6-K)\,C^2-M]\frac{f_0}{C}\right\}$$
$$+[(3K-5)+MC^{-2}]\frac{\partial^2 f_0}{\partial \tau_0^2}, \tag{12}$$

where $\quad H = r^2+1,\quad K = \tfrac{1}{4}r^2+\tfrac{7}{2}+(1/4r^2),\quad M = 1+r^{-2}.$

This equation has to be solved with an appropriate initial condition, subject to regularity at $C = 0$ and ∞.

As time T advances the solution must approach the steady-state distribution

$$f^*(C) = f_0(C,\tau_0,\infty) = \text{constant}\times C[(HC^4+KC^2+M)F]^{-\frac{3}{4}}, \tag{13}$$

where

$$F = \left[\frac{2HC^2+K-(K^2-4HM)^{\frac{1}{2}}}{2HC^2+K+(K^2-4HM)^{\frac{1}{2}}}\right]^{(4-K)/(K^2-4HM)^{\frac{1}{2}}}\qquad (K^2 > 4HM),$$

plus the obvious analytic continuation when K^2 does not exceed $4HM$ (Hinch & Leal 1972). The constant in (13) is determined from the normalization of N, which reduces to the integral condition

$$\int_0^\infty dC \int_0^{2\pi} d\tau_0 f_0(C, \tau_0, T) = \tfrac{1}{2}.$$

As we shall see, (12) is also applicable to the function f_1 in the solution (10) for the step-up problem, although a different final steady solution will be attained in that instance.

To discuss the decay of the difference between the initial conditions and the final state, we must look at the eigenvalue problem associated with (12). For an eigensolution

$$f_0(C, \tau_0, T) = f(C)\, e^{-\lambda T + in\tau_0}$$

the eigenfunction is governed by

$$\frac{d}{dC}\left\{[HC^4+KC^2+M]\frac{df}{dC}+[2HC^4+(6-K)\,C^2-M]\frac{f}{c}\right\} + \{2\lambda - n^2[3K-5+MC^{-2}]\}f = 0 \qquad (14)$$

subject to regularity conditions at $C = 0$ and ∞. Except for the trivial case of spheres ($r = 1$) and zero eigenvalue which corresponds to the steady solution (13), no closed-form analytic solutions have been found for (14). We shall concentrate our attention on the limiting case $r \gg 1$, where certain general properties of the eigenfunctions and eigenvalues may be determined which will enable the qualitative features of the rheological behaviour to be deduced. The eigenvalues for the other limit $r \ll 1$ can be obtained by interchanging r and r^{-1}.

A uniformly valid approximation to (14) for large r is

$$\frac{d}{dC}\left\{\left(C^2+\frac{4}{r^2}\right)\left[(4C^2+1)\frac{df}{dC}+(8C^2-1)\frac{f}{C}\right]\right\}+\left\{\frac{8\lambda}{r^2}-n^2\left(3+\frac{4}{C^2r^2}\right)\right\}f = 0. \qquad (15)$$

In order to ascertain the nature of the eigenfunctions we consider three ranges of C. First, at one end of the domain where $0 \leqslant C \ll r^{-1}$, equation (15) reduces to

$$\frac{d}{dC}\left[\frac{df}{dC}-\frac{f}{C}\right]-\frac{n^2}{C^2}f = 0.$$

To ensure regularity for $C \to 0$, we select the solution proportional to C^{1+n}, rather than $C \ln C$, for $n = 0$ and C^{1-n} for $n \geqslant 1$. At the other end, where $C \gg 1$, equation (15) takes the form

$$\frac{d}{dC}\left[C^4\frac{df}{dC}+2C^3 f\right] = 0,$$

with solutions C^{-2} and C^{-3}. The regularity condition at $C = \infty$ comes from the need to construct an eigensolution on the whole orientation space. The eigenfunction must be either symmetric or antisymmetric about the x_1, x_2 plane ($C = \infty$). This implies that the eigenfunction $f(C)$ should be either $C^{-2}+O(C^{-4})$ or $C^{-3}+O(C^{-5})$ as $C \to \infty$. Finally, in the important intermediate region $r^{-1} \ll C \ll 1$, equation (15) becomes

$$\frac{d}{dC}\left[C^2\frac{df}{dC}-Cf\right]+\left(\frac{8\lambda}{r^2}-3n^2\right)f = 0.$$

This has a solution

$$f = \cos [((8\lambda/r^2) - 1 - 3n^2)^{\frac{1}{2}} \ln C + \text{constant}]. \tag{16}$$

Now the mth eigenfunction must have m zeros within the domain of definition. Since the present eigenfunction is single-signed in the two end regions, the m crossings of zero must occur in the intermediate region $r^{-1} \lesssim C \lesssim 1$ where expression (16) approximately applies. This gives an asymptotic estimate of the eigenvalues of

$$\frac{r^2}{8}\left\{1 + 3n^2 + \left(\frac{(m+\delta)\pi}{\ln r}\right)^2 \left(1 + O\left(\frac{1}{\ln r}\right)\right)\right\}, \tag{17}$$

in which the end effects are confined to the function δ, which depends on n and weakly on m as in the group $m/\ln r$. The preceding arguments can be formally justified by employing the method of matched asymptotic expansions. An inner region of $O(r^{-1})$ is required at $C = 0$, while the expansion is made in the two small parameters r^{-1} and $(\ln r)^{-1}$. The inner functions are related to Legendre functions.

The estimate (17) is the primary result of this section, but it is clearly based on a number of assumptions about the structure of the eigenfunctions. A numerical verification of the asymptotic form of the eigenfunctions is not easy: by the time r is large enough for $\ln r$ to be large, the small region $0 \leqslant C \leqslant r^{-1}$ cannot be resolved well by a finite difference scheme. A numerical integration of (14) for the lower modes $(n, m = 0, 1, 2)$ has, however, found the eigenvalue estimate (17) to be about 10 % inaccurate at $r = 4$ and within 5 % by $r = 8$, using $\delta = 1{\cdot}1$, $1{\cdot}5$ and $1{\cdot}9$ for the even modes at $C = \infty$ and $\delta = 1{\cdot}6$, $2{\cdot}0$ and $2{\cdot}4$ for the odd modes with $n = 0$, 1 and 2 respectively. No substantial increase in accuracy was found up to $r = 128$, perhaps owing to the slow decay of the logarithmic factors.

5. Start of a steady shear

The results of the previous section are now applied to the rheological response of a suspension of rod-like particles $(r \gg 1)$ when a steady strong shear flow starts from a state of rest, i.e.

$$\gamma(t) = \begin{cases} 0 & (t < 0), \\ \gamma = \text{constant} & (t > 0), \end{cases} \tag{18}$$

with $D/\gamma \ll 1$. We assume that the orientation distribution is initially uniform so that the initial conditions on the drift functions $f_n(C, \tau_0, T)$ which occur in the homogeneous solution at each level of the expansion are simply

$$f_0(C, \tau_0, 0) = [4\pi g(C, \tau)]^{-1}|_{\tau=\tau_0}, \tag{19a}$$

$$f_n(C, \tau_0, 0) = 0 \quad (n \geqslant 1). \tag{19b}$$

We confine our attention to the first approximation to N. In spite of the fact that the necessary eigenfunctions are not explicitly available, a reasonably complete qualitative description of N_0, and hence the bulk stress, can be pieced together from the estimate (17) of the eigenvalues plus a consideration of the short time scale $T \ll 1$ on which there is no diffusion. Okagawa (1972, private com-

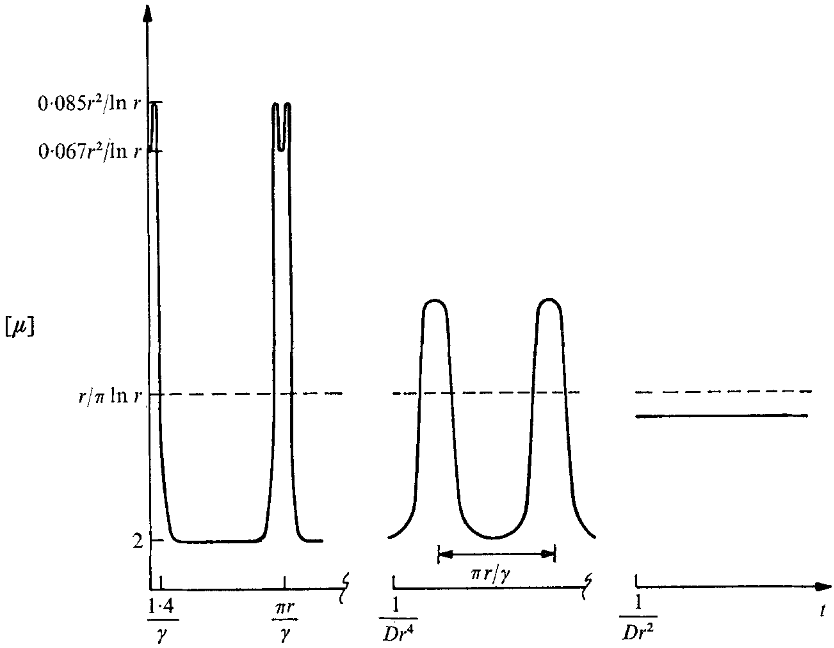

FIGURE 1. The intrinsic viscosity after the start of a steady shear.

munication) has independently investigated a portion of the non-diffusive regime using both theoretical calculations and very interesting experimental observations.

The effective viscosity

We begin our discussion of the rheological behaviour by considering the time variations of the intrinsic viscosity. It is convenient to separate the development into three stages, $t \lesssim (Dr^4)^{-1}$, $(Dr^4)^{-1} \lesssim t \lesssim (Dr^2)^{-1}$ and $t \gtrsim (Dr^2)^{-1}$, as shown in figure 1.

The first is the short time scale $T \ll 1$ on which f_0 is essentially unchanged from (19a). Combining this distribution with (3), the intrinsic viscosity during this stage can be expressed as

$$[\mu] = 2+\frac{r^5}{2\pi\ln r}\int_0^\infty dC\int_0^{2\pi} d\tau\,\frac{C^5\sin^2\tau\cos^2\tau}{[1+C^2+C^2r^2\sin^2\tau]^2}\,\frac{1}{[1+C^2+C^2r^2\sin^2(\tau-\omega t)]^{\frac{3}{2}}}, \tag{20}$$

where the τ_0 transformation is simply $\tau_0 = \tau-\omega t$ with $\omega = \gamma r/(r^2+1)$. This function is periodic with sharp peaks at $\omega t = n\pi$. Between the peaks it can be evaluated analytically to yield

$$[\mu] = 2+(\cot^2\omega t/\ln r). \tag{21a}$$

The nature of the peaks is found by noting they occur for ωt within $O(r^{-1})$ of $n\pi$, i.e. for $\tau_0 = \tau-n\pi-\delta/r$, where δ is of order unity. Then

$$[\mu] = \frac{r^2}{\pi\ln r}\int_0^\infty dC\int_{-\infty}^\infty ds\,\frac{C^5(s+\delta)^2}{[1+C^2+C^2(s+\delta)^2]^2}\,\frac{1}{[1+C^2+C^2s^2]^{\frac{3}{2}}}. \tag{21b}$$

For $\delta = 0$ the integration can be carried out analytically, yielding the initial value

$[\mu] = r^2/15 \ln r$. For other values of δ the integration is most conveniently done numerically. A maximum value of $[\mu]$ equal to $0{\cdot}085 r^2/\ln r$ is found at

$$\gamma t - n\pi r = \delta = \pm 1{\cdot}4.$$

This is the split peak shown in figure 1 at each $\omega t = n\pi$.

The strong oscillation of $[\mu]$ is a consequence of the nature of the Jeffery orbits for large r together with the initial uniform state. For large r each particle spends most of its orbit with its axis of rotation virtually aligned with the flow. In this position the disturbance caused by the particle is minimized and hence also its contribution to the intrinsic viscosity. When not aligned a particle causes a much stronger $O(r^2)$ disturbance. At the initial instant the particle orientation is random. Thus, most of the particles are in the little frequented non-aligned positions and the intrinsic viscosity is large. The peak quickly diminishes and the intrinsic viscosity takes on the value 2 as the particles align with the flow for an extensive period. The further peaks occur when the particles flip through 180° to the opposite alignment at each half orbit period. The double peak is a result of the maximum dissipation that occurs when the average particle orientation coincides with the two directions of the principal extension in the undisturbed shear. We note that the value of $[\mu]$ averaged over an orbit period must be the Einsenschitz value $r/\pi \ln r$ in this first stage.

The effects of Brownian diffusion are confined to the second and third stages and consist of two separate effects: a redistribution of the relative population of the various orbits and a phase mixing about each orbit. We have already given an estimate, equation (17), of the eigenvalues associated with the drift of N_0 on the long time scale T. Since the initial form of (19 a) of f_0 has a period $\tau = \pi$ the excited eigenmodes are those with even values of n. Without an explicit resolution of the initial distribution into the eigenfunctions it is not possible to be precise as to the weight of any particular mode. However, in view of the $O(r^{-1})\ \tau_0$ breadth of the peak in the initial N_0 (and hence the variation of $[\mu]$ in time), it is clear that all the even modes up to $n = O(r)$ must be included with essentially the same weight. The weights of the higher modes $n > O(r)$ fall off rapidly. The longest relaxation time of the distribution is thus $8/Dr^2$, and corresponds to a redistribution of the relative population of the various orbits. On the other hand, the important long tail of the harmonics out to $n = O(r)$ is affected on the much shorter time scale $O(Dr^4)^{-1}$. This quicker diffusion process is dominated by the phase mixing about the orbits. The intrinsic viscosity in these two diffusion stages is sketched in figure 1. The phase mixing in the middle stage at $t = O(Dr^4)^{-1}$ causes the peaks to decrease in magnitude, broaden and lose their double humped character. In the final stage at $t = O(Dr^2)^{-1}$ the last (lowest) harmonics of the oscillation decay away, and owing to the adjustment in the relative orbit distribution the averaged viscosity decreases slightly from Eisenschitz value to the steady-state value $0{\cdot}315153 r/\ln r$ (Hinch & Leal 1972). It is ironic that these values are within 1 %.

The normal stress differences

In the steady state the normal stress differences are of $O(D)$ for $D \ll 1$. We find in this section that the transients which arise from N_0 are cf the same magnitude

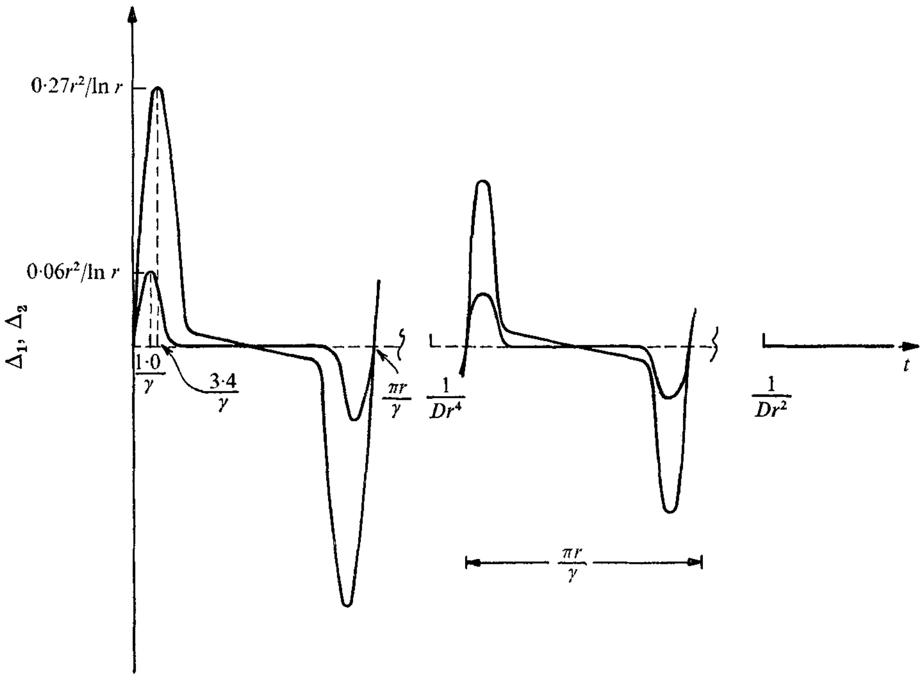

FIGURE 2. The normal stress differences after the start of a steady shear. The curve with the lower peaks refers to the second normal stress.

as the particle contribution to the shear stress. We have sketched the principal and secondary normal stress differences as functions of time in figure 2. Again there are three stages of development corresponding to pure advection and diffusion through phase mixing of the high and low harmonics.

The principal and secondary stress differences in the initial advection stage ($T \ll 1$) can be expressed as

$$\Delta_1 = \frac{\sigma_{11}-\sigma_{33}}{\mu\Phi\gamma} = \frac{r^2}{\pi \ln r}\int_0^\infty dC \int_0^{2\pi} d\tau \times \frac{C^3 r^2 \sin\tau\cos\tau\,(C^2r^2\sin^2\tau - 1)}{(1+C^2+C^2r^2\sin^2\tau)^2\,[1+C^2+C^2r^2\sin^2(\tau-\omega t)]^{\frac{3}{2}}}, \tag{22a}$$

$$\Delta_2 = \frac{\sigma_{22}-\sigma_{33}}{\mu\Phi\gamma} = \frac{r^2}{\pi \ln r}\int_0^\infty dC \int_0^{2\pi} d\tau \times \frac{C^3 r^2 \sin\tau\cos\tau\,(C^2\cos^2\tau - 1)}{(1+C^2+C^2r^2\sin^2\tau)^2\,[1+C^2+C^2r^2\sin^2(\tau-\omega t)]^{\frac{3}{2}}}. \tag{22b}$$

As was the case with the intrinsic viscosity, the functions Δ_1 and Δ_2 both show sharp periodic peaks, separated by $t = r\pi/\gamma$, which are associated with the concerted flip of the particles from one aligned state to another. Unlike the intrinsic viscosity, which oscillates about a non-zero mean, the average values of Δ_1 and Δ_2 are zero to $O(1)$ in $D \ll 1$. The change in sign occurs when the particles pass from being on average in the quadrants of compressional strain to the extensional quadrants. The expressions for Δ_1 and Δ_2 can be evaluated analytically between the peaks:

$$\Delta_1 = (r/2\ln r)\cot \omega t, \tag{23a}$$

$$\Delta_2 = O(1/\ln r), \tag{24a}$$

i.e. the secondary difference is smaller by $O(r^{-1})$. The nature of the peaks is again ascertained by putting $\tau_0 = \tau - n\pi - \delta/r$:

$$\Delta_1 = \frac{2r^2}{\pi \ln r}\int_0^\infty dC \int_{-\infty}^\infty ds \frac{C^3(s+\delta)\,[C^2(s+\delta)^2-1]}{[1+C^2+C^2(s+\delta)^2]^2\,[1+C^2+C^2s^2]^{\frac{3}{2}}}, \tag{23b}$$

$$\Delta_2 = \frac{2r^2}{\pi \ln r}\int_0^\infty dC \int_{-\infty}^\infty ds \frac{C^3(s+\delta)\,(C^2-1)}{[1+C^2+C^2(s+\delta)^2]^2\,[1+C^2+C^2s^2]^{\frac{3}{2}}}, \tag{24b}$$

i.e. Δ_1 and Δ_2 are of the same order of magnitude. In addition we note that because Δ_1 and Δ_2 are both odd in δ the split positive maxima in $[\mu]$ become peaks

$$\Delta_1 = \pm 0{\cdot}27r^2/\ln r \quad \text{and} \quad \Delta_2 = \pm 0{\cdot}061r^2/\ln r$$

at

$$\gamma t - n\pi r = \delta = \pm 3{\cdot}4 \text{ and } \pm 1{\cdot}0,$$

respectively.

The effects of Brownian diffusion in the remaining two stages are qualitatively similar to those described in the previous section for $[\mu]$, although only phase mixing is relevant to the normal stresses. The peaks begin to decrease and broaden at $t = O(Dr^4)^{-1}$. The last few harmonics decay away at $t = O(Dr^2)^{-1}$, leaving the steady normal stresses which are $O(Dr^3)$ smaller than the steady shear stress.

6. Step change in shear rate

As a second example we have carried out similar calculations to those described in the previous section for the step up from one steady strong shear to another:

$$\gamma(t) = \begin{cases} \gamma_- & (t < 0), \\ \gamma_+ & (t > 0). \end{cases} \tag{25}$$

We again confine our attention to the limit of large r. Although this problem differs only from the start up in the initial condition, the rheological response is considerably different.

The key to the present example is the observation that except for the multiplicative factor γ^{-n} in N_n the form of the steady solutions N_n is independent of the shear rate. A step change in the shear rate will therefore not alter the orientation distribution at all to first order, the transients being confined to N_1 and higher orders; thus

$$N_0 = f^*(C)\,g(C,\tau)$$

for all times, where $f^*(C)$ is given by (13). The equation governing N_1 is (8*b*), which is solved in equation (10). In an earlier paper (Hinch & Leal 1972) we found the integral contribution to (10) with $\partial f_0/\partial T = 0$. For large r it is

$$\frac{1}{\gamma}\frac{N_1^*}{g} = \frac{1}{\gamma}\frac{15r^3}{\pi}\frac{C^5}{(4C^2+1)^{\frac{7}{2}}}\sin 2\tau\,(1-\cos 2\tau). \tag{26}$$

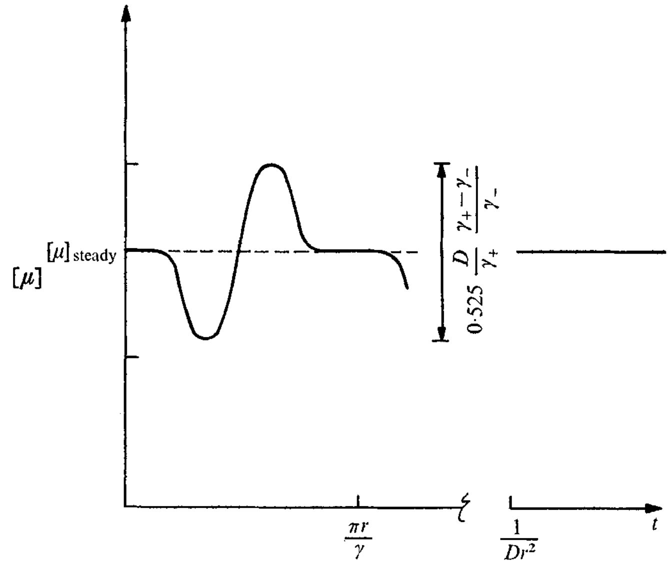

FIGURE 3. The intrinsic viscosity after the step increase in steady shear.

The initial condition on the homogeneous drift function $f_1(C, \tau_0, T)$ is thus

$$f_1(C, \tau_0, 0) = \left(\frac{\gamma_+ - \gamma_-}{\gamma_+ \gamma_-}\right)\left[\frac{N_1^*}{g}\right]_{\tau=\tau_0}. \tag{27}$$

The drift of f_1 is governed by the secularity condition which occurs at the $O(D^2)$ approximation. This equation is identical to equation (9) for f_0 because the steady forced component N_1^* is odd in τ and so makes no contribution, i.e.

$$\int_0^{2\pi} g^{-1} \nabla^2_{C,\tau,\tau_0} N_1^* \, d\tau = 0.$$

The homogeneous solution f_1 may therefore be expanded in the eigenmodes discussed in § 4.

Since N_0 is not changed, the intrinsic viscosity is constant at its steady-state value to first order in D. A transient oscillation does appear at $O(D)$, dominating the $O(D^2)$ corrections to the steady value. The normal stresses, which are of $O(D)$ in the steady state, show transient oscillations at the same order owing to the oscillations in N_1. We have sketched the behaviour of the intrinsic viscosity and the normal stress functions Δ_1 and Δ_2 in figures 3 and 4.

In the first stage, $T \ll 1$, the relatively simple form of (26) in (27) allows analytic evaluation of the rheological quantities:

$$[\mu] = [\mu]_{\text{steady}} + \frac{D}{\gamma_+}\frac{\gamma_+ - \gamma_-}{\gamma_-} 0{\cdot}101 \frac{r^4}{\ln r}[\sin 4\omega t - 2\sin 2\omega t], \tag{28a}$$

$$\Delta_1 = \frac{\sigma_{11} - \sigma_{33}}{\mu\Phi\gamma} = \frac{D}{\gamma_+}\frac{1}{4}\frac{r^4}{\ln r}\left[1 + \frac{\gamma_+ - \gamma_-}{\gamma_-}(2\cos 2\omega t - \cos 4\omega t)\right], \tag{28b}$$

$$\Delta_2 = \frac{\sigma_{22} - \sigma_{33}}{\mu\Phi\gamma} = \frac{D}{\gamma_+}\frac{\gamma_+ - \gamma_+}{\gamma_-} o\left(\frac{r^4}{\ln r}\right). \tag{28c}$$

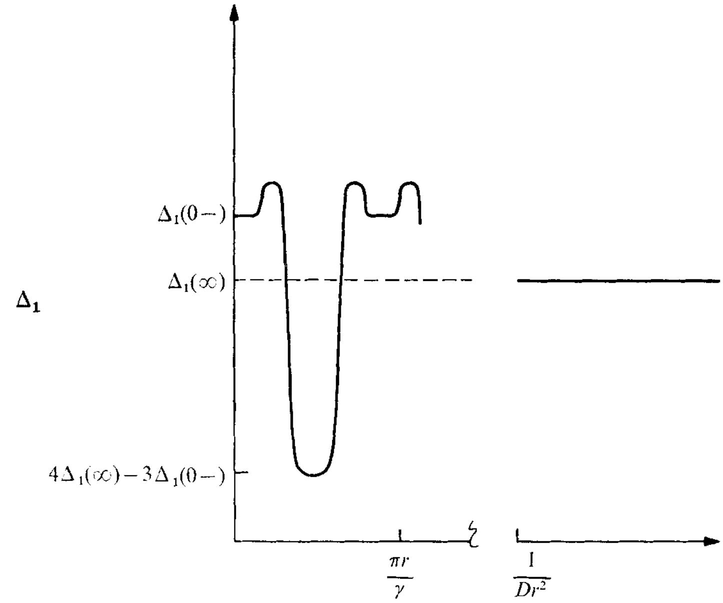

FIGURE 4. The primary normal stress difference after a step decrease in steady shear.

All the rheological quantities oscillate at frequencies equal to or twice the inverse orbit period, with magnitudes proportional to the fractional change in the shear rate. The secondary normal stress difference is asymptotically smaller than the primary difference.

The effects of Brownian diffusion are simpler in the present case than in the start-up problem. Because of the special form of the initial state, the only excited eigenmodes for the drift of f_1 have $n = 2$ and $n = 4$. Thus, the time scales for the diffusive decay of the oscillations are estimated from (17) as $8/13Dr^2$ and $8/17Dr^2$, corresponding to phase mixing.

7. Conclusions

It is useful to compare the results of the present investigation for particles with $r \gg 1$ with those obtained in our previous study of nearly spherical particles. [Except for some rescaling, the results for $r \ll 1$ are obtained from the large r limit by substituting r^{-1} for r.] Two intrinsic time scales were observed for a suspension of near spheres: Ω^{-1} due to rotation about the Jeffery orbits, and $(6D)^{-1}$ due to Brownian diffusion. These features are unchanged for stress relaxation as is shown in § 2. However, in the presence of a non-zero shear, the anisotropy of the suspension associated with the non-spherical particles leads to quantitative changes in both the oscillations and their decay.

The frequency of the oscillation due to the orbit rotation decreases with the increasing Jeffery orbit period $2\pi(r+r^{-1})/\gamma$. As the rotation rate becomes non-uniform, i.e. as the particle spends a long period of quiescent alignment followed by a rapid disturbing flip-over, the oscillations can become spiked with long intermediate periods of a nearly constant bulk stress.

The decay rate of the transients is enhanced by the presence of large gradients in the distribution. Because the particles spend most of their orbit period within $O(r^{-1})$ of alignment with the flow, the typical gradients must be at least of $O(r)$. Thus the diffusion rate increased to $O(Dr^2)$. Larger gradients of $O(r^2)$ result from the uniform initial condition as the particle rotation rate reduces during the orbit from the initial γ to the long period of γr^{-2}.

Although we have confined ourselves to a particularly simple class of time-dependent behaviour, namely the transients in a constant strong shear flow, we believe that the results are indicative of the response of the anisotropic suspension in more general circumstances.

This work was carried out while E. J. H. was a visitor in Applied Mathematics at the California Institute of Technology. L. G. L. was partially supported by grant 6489-AC 7 from the Petroleum Research Fund, administered by the American Chemical Society.

REFERENCES

Hinch, E. J. & Leal, L. G. 1972 *J. Fluid Mech.* **52**, 683.
Leal, L. G. & Hinch, E. J. 1971 *J. Fluid Mech.* **46**, 685.
Leal, L. G. & Hinch, E. J. 1972 *J. Fluid Mech.* **55**, 745.